EXPERIMENTAL STUDY ON AMPLITUDE-FREQUENCY CHARACTERISTIC AND BASIN STABILITY OF HORIZONTALLY DRIVEN PENDULUM

Ji Jia

School of Science, Beijing University of Posts and Telecommunications, Beijing, China

Ye Wu

School of Science, Beijing University of Posts and Telecommunications, Beijing, China
State Key Lab of Information Photonics and Optical Communications, Beijing University of Posts and Telecommunications, Beijing, China

Weiqing Liu

School of Science, Jiangxi University of Science and Technology, Ganzhou, China

Jinghua Xiao

School of Science, Beijing University of Posts and Telecommunications, Beijing, China
State Key Lab of Information Photonics and Optical Communications, Beijing University of Posts and Telecommunications, Beijing, China; e-mail: jhxiaobupt@163.com

In this article, an inverted pendulum system is set up to explore the dynamics of a horizontally driven pendulum which exhibits a great variety of dynamical behavior and appears in a wide range of applications in the field of engineering. The facility is efficient to experimentally explore two kinds of coexisting movement patterns in the horizontally driven pendulum, i.e. in-phase and anti-phase patterns between the angular velocity of the pendulum rod and the direction of the driving forces. Theoretical analysis is applied to reveal the regimes of the coexistence of the two movement patterns, which is promising to control the system to a desired pattern.

Keywords: horizontally driven pendulum system, bifurcation, basin stability

1. Introduction

The study of pendulum motion is a classical problem in physics since it reveals the basic movement in the world of nature (Mokha *et al.*, 1991; Wu *et al.*, 2012a), ranging from physics, chemistry ecology and economics to biology (Wu *et al.*, 2012b). Without additional driving and damping, an isolated pendulum swings in a simple period mode. With various types of additional driving and damping, driven pendulum models are widely used since they often capture the key dynamics of many complicated dynamical systems (Leven and Koch, 1981; Sauer *et al.*, 1999; Masoud *et al.*, 2004). For instance, through vertical shaking of the pendulum pivot point, a lot of chaotic motions are observed in the driving pendulum (Heng and Martienssen, 1992; Baker, 1995). However, a group of pendulums driven by horizontal forces has been recently examined in experiments and widely applied in engineering (Thakur *et al.*, 2008), yet the basic dynamical behavior is still unclear and need further concentrations. The most noteworthy is that horizontal driving may lead the pendulum to angular vibration of a non-zero mean value (Schmitt and Bayly, 1998) and a variety of dynamical characteristics such as the existence of bi-stability (Nakamura *et al.*, 2011; Yan *et al.*, 2012).

A series of equipment such as driving stepper motors, poles of metal and conveyor belts are used to set up the device. It can be observed in the experiment that the special parameters

lead the top and bottom ends of the rod of the pendulum to in-phase or anti-phase oscillating. In our experiment, the amplitude-versus-frequency curve is studied, dynamic analysis of the system and numerical simulation is carried out, and the basins and their stability of the two coexisting periodic oscillation states are considered. Moreover, it is noticeable that there is a certain difficulty to control the switching between the two coexisting movement patterns. In reaction of this phenomenon, a possible explanation is given in theory, and it is hopeful to benefit for more experiments and applications.

This paper is arranged as follows. In Section 2, the experimental setup is introduced. In Section 3, we present the experimental results and analysis. In Section 4, the theoretical model and analysis are introduced in detail. The results of numerical simulations are presented in Section 5. Finally, in Section 6, we recommend some other significant applications and draw a conclusion.

2. Experimental setup

A schematic of the physical pendulum system we consider, as shown in Fig. 1, consists of an inverted pendulum system and an acquisition system linked with a computer. The system is mainly composed of a driving stepper motor, conveyor belt, horizontal track, slider, and swinging rod. The slider is confined on the horizontal track and can move freely in the direction of the horizontal track. Applying a sine signal to the driving motor, the slider may exhibit a simple harmonic movement in the direction of the horizontal track through the conveyor belt connected to the motor. The swinging rod connected with the slider through a rotating axis (perpendicular to the trace of the slider) can swing freely in the vertical plane.
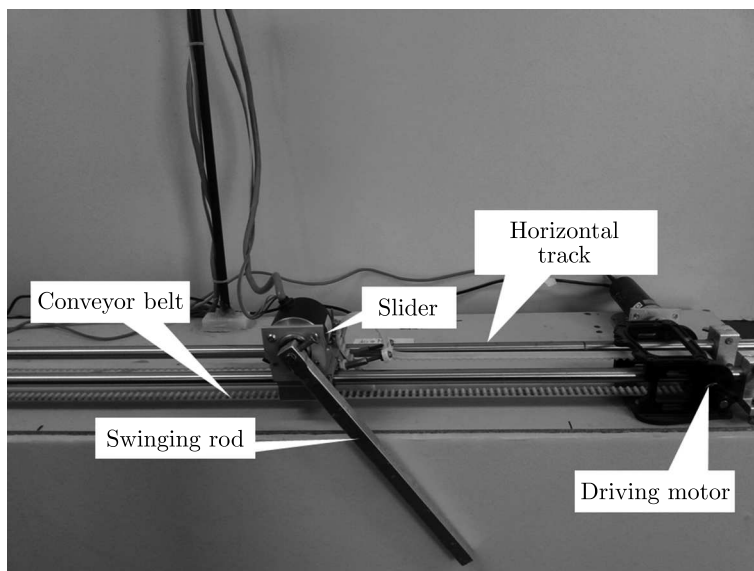

Fig. 1. Experimental setup

Several sensors are set up on the rotating axis. The sensors record the data of the rotating angle of the rotating axis and the horizontal displacement of the slider, and then transmits those data to the computer for further analysis (Wu *et al.*, 2014). The corresponding experimental parameters are set as follows. Length of the rod is 0.193 m, and the driving frequency varies from 0.6 Hz to 2.0 Hz. The time interval of acquisition is 0.01 s.

3. Experimental results and analysis

Under driving with the sine signal, the movements of the slider and the swinging rod are coupled together. To describe the movement of the slider and the swinging rod, the displacement $x(t)$ and the angular displacement $\theta(t)$ are defined by selecting the balance point of the simple harmonic movement and the vertical line through the rotor axis as a reference, respectively. The time series of the displacement $x(t)$ and the angular displacement $\theta(t)$ recorded by the sensors reveal the dynamics of the slider and the swinging rod as shown in Fig. 2a,b. Two kinds of movement patterns are observed as (a) in-phase pattern, and (b) anti-phase pattern for different initial values. When the coupled movement is in the in-phase (anti-phase) pattern, the slider and the swing rod move in the same (opposite) directions.
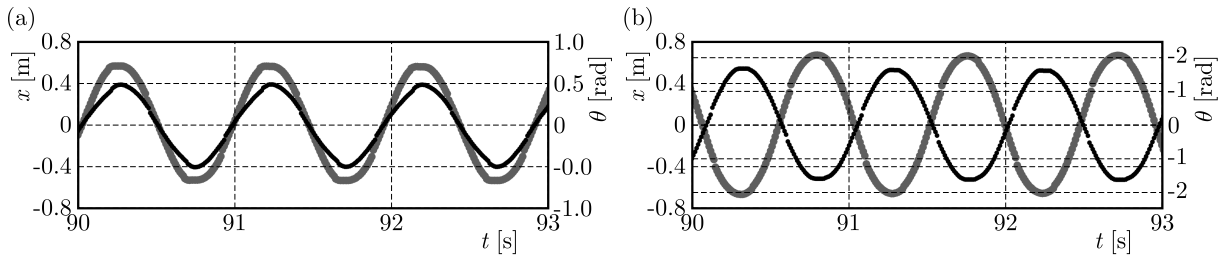

Fig. 2. Time series of the horizontal displacement of the slider (expressed by x and plotted by the thin black line) and the pivot angle of the rod (expressed by θ and plotted by the thick gray line).
(a) In-phase oscillation state with the initial value $(x, \theta) = (0.93, 0.52)$, (b) anti-phase oscillation state with the initial value $(x, \theta) = (-0.49, 1.74)$

According to the experimental set up, the driving signal has obvious influence on the amplitude of the movement of the slider and the swinging rod. To reveal the effects of the frequency of the driving signals on the movements, the amplitude-frequency characteristics of the driven oscillators are recorded. Since there are two coexisting patterns, it is necessary to check if the amplitude-frequency curves of those two patterns are different. The maximal swing angle of the rod is recorded for all given frequencies of the driving signal as shown in Fig. 3. Interestingly, in a particular range of the parameter $f \in [0.722, 1.139]$, there are two quite different amplitude-frequency curves for different patterns. When the system is in the anti-phase pattern, the maximal swing angle is quite larger than that when the system is in the in-phase pattern.
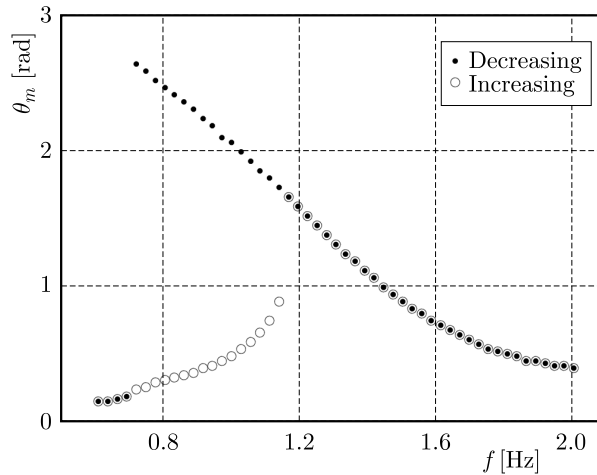

Fig. 3. Amplitude-frequency curves of the horizontally driven pendulum. The circles and dots denote the increasing and decreasing processes of frequency, respectively

4.   Theoretical model

We consider a horizontally driven pendulum system whose rotation axis is driven by a horizontal force. The rod is rigid and uniform, the mass is m, and the length is l. The upper end is fixed on a slider which can move horizontally at a particular rate along the track when driven by a motor. A model diagram is shown in Fig. 4.
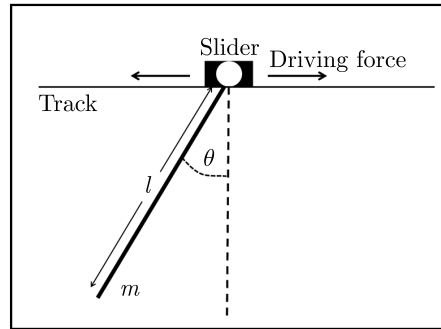

Fig. 4. Sketch of the model. A rod of mass m and length l is subjected to a horizontal driving force and angular displacement θ from the vertical direction

We control the driving signal of the driving motor and let the speed of the slider satisfy the following equation

$$\dot{x}(t) = A_m \sin(2\pi f t) \tag{4.1}$$

where A_m is the maximum value of the speed and f is the frequency of driving force. When the slider moves at the speed $\dot{x}(t)$ in equation (4.1), the rod hinged in the slider will swing according to the driving signal. The equation of dynamics of the system can be written as the following Euler-Lagrange equation

$$L = \frac{1}{2}m\left(\dot{x}^2 + \frac{1}{3}l^2\dot{\theta}^2 + \dot{x}l\dot{\theta}\cos\theta\right) - \frac{1}{2}mgl(1 - \cos\theta) \tag{4.2}$$

As a consequence, the kinematical equation of the system can be expressed as a second order nonlinear differential equation

$$\frac{1}{3}ml^2\ddot{\theta} + \pi f ml A_m \cos(2\pi f t)\cos\theta + \frac{1}{2}mgl\sin\theta + C\dot{\theta} = 0 \tag{4.3}$$

In equations (4.2) and (4.3), m and l are the mass and length of the rod respectively, θ is the swing angle of the rod, g is the acceleration of gravity, and C is the damping coefficient.

5.   The results of numerical simulations

5.1.   In-phase and anti-phase periodic oscillation

There are four parameters to be confirmed in equation (4.3). In order to ensure the simulation results coincide with the experimental data, the parameters should be measured as accurately as possible. The mass and length of the rod can be directly measured and the results are $m = 0.05631$ and $l = 0.193$ (in SI). The maximum speed of the slider can be precisely adjusted by the computer and the value is fixed as $A_m = 0.3544$ so that the moving slider can be kept in a proper range. Comparing the numerical simulation repeatedly with experimental results is necessary to confirm the damping coefficient. Without the horizontal driving force, the system is underdamped. If the rod is released from the horizontal direction, it will oscillate for a few

periods and end up vertically stationary due to the action of damping. Through experiments, we record the duration of the underdamped system and the number of times the rod passesthe stable point. Thus, it can be found in the simulation after several repeated attempts that for the damping coefficient is $C = 0.001$, the number of oscillations and the total time of the motion are both consistent with the experimental results. Hence, the above values are determined to be used in our following simulations.

We obtain the dynamics under different initial conditions by numerical calculation based on the 4th-order Runge-Kutta method. There is also a coexistence of the in-phase and anti-phase patterns in the system as shown in Fig. 5. The numerical results excellently agree with the experimental phenomena given in Fig. 2. Figures 5a and 5b are numerical results of time series of the in-phase and anti-phase oscillation state, respectively.
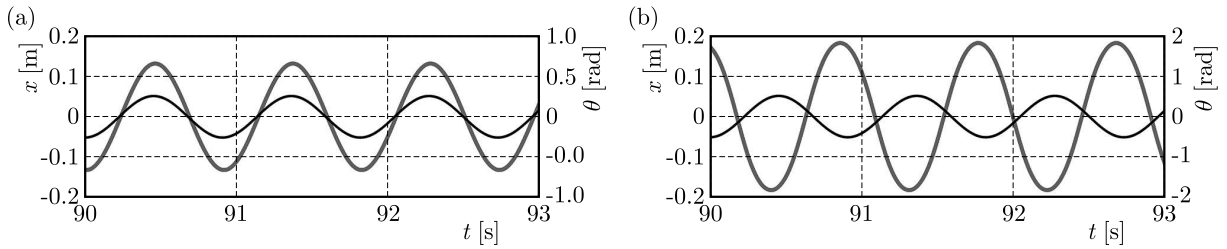

Fig. 5. Numerical simulation results of two kinds of the oscillation state. The displacement of the top end of the rod is plotted by the thin black line and the pivot angle of the rod is plotted by the thick grey line. (a) The in-phase oscillation state, (b) the anti-phase oscillation state

5.2. Bifurcation phenomenon

Let us consider the amplitude-frequency curve of the horizontally driven pendulum system numerically. We record the maximal values of the swing angle of the rod with a quasi-static method, i.e. we start from the driving frequency $f = 0.7$ Hz (2.0 Hz), then slightly increase (decrease) the driving frequency and take the final states with tiny noise as the initial value for a new f. Since there are two coexisting states when $f = 0.7$ Hz, two branches of the amplitude-frequency curves can be obtained. Compared with the amplitude-frequency of the experimental results, the numerical one coincides with the experimental one well as shown in Fig. 6. The black solid line and the grey dashed line are the numerical results while the black triangles and the grey circles are experimental results.

Furthermore, the final state of the horizontally driven pendulum system is so sensitive to the initial values that obvious uncertainty and unpredictability exist in the experiment. Two very closing initial values may lead to quite different states. It is extremely difficult to make the initial values exactly the same when repeating the practical experiments. There is always a slight difference and interference during the experiments. Therefore, prediction and control of the final state of the system become a noteworthy problem in the experiment.

5.3. Basin and its stability

It is meaningful to explore the basin stability of the two coexisting patterns since detailed information of the basin stability is important in predicting the dynamical fate of the coupled system. With the fixed parameters $l = 0.193$, $A_m = 0.3544$, $C = 0.001$, $f = [0.607, 1.1763]$ Hz, the system has two coexisting patterns (in-phase or anti-phase patterns). To observe the basin of those two coexisting patterns in detail, we recorded and dotted all initial values $(\theta_0, \dot{\theta}_0)$ with which the system finally transits to the in-phase pattern for a given driving frequency f. According to the results shown in Figs. 7a-7h, one may find that the basins of the two patterns
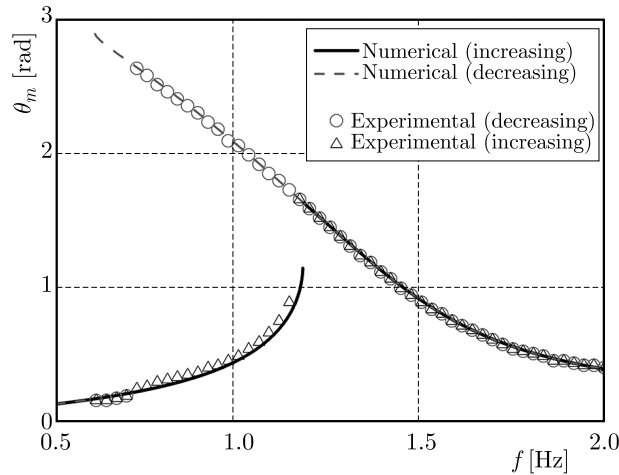
Fig. 6. Amplitude-frequency curves of the numerical and experimental results. The upper branch is for the anti-phase oscillation state, and the lower branch if for the in-phase state. The triangles (increasing) and circles (decreasing) are the experimental results while the solid (increasing) and dash (decreasing) lines are the numerical ones
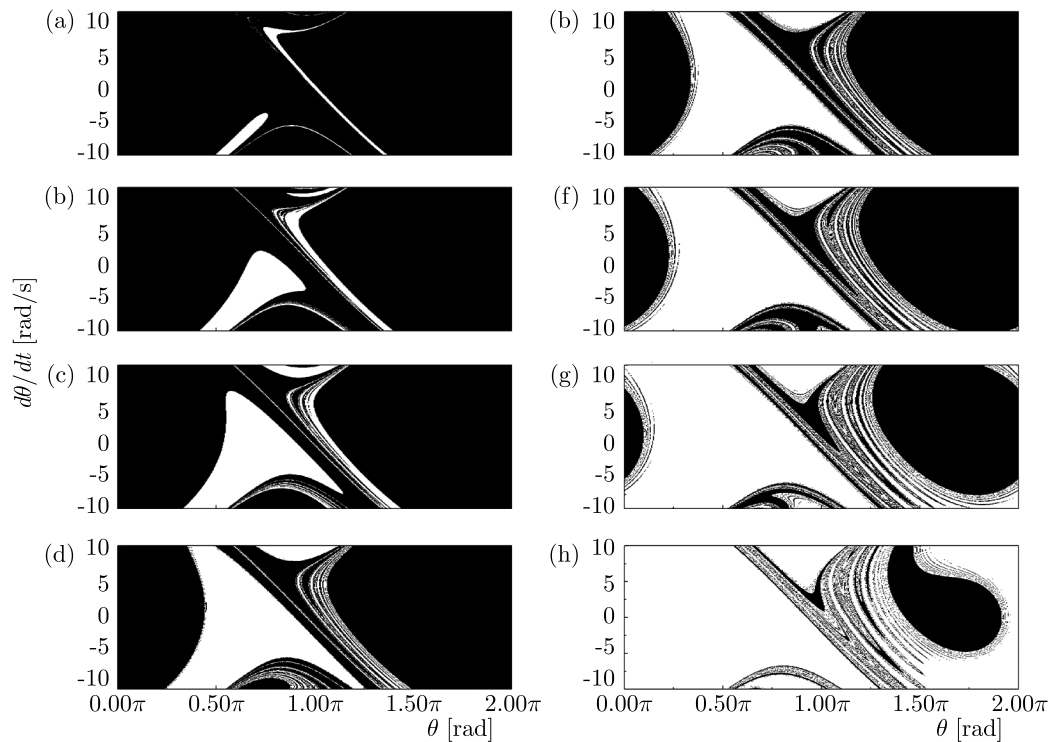

Fig. 7. Basins of the system with different frequencies. From (a) to (h), the driving frequency of the system changes from $0.8\,\mathrm{Hz}$ to $1.15\,\mathrm{Hz}$ by step of $0.05\,\mathrm{Hz}$

are possible and riddled in some phase space of $(\theta, \dot{\theta})$. Moreover, with an increment in the driving frequency, the basins of the in-phase pattern shrink with that of the anti-phase one expanding.

With detailed information on the basin, it is helpful to determine the final state of the bistable system in the sense of the control experiment. Since is convenient to set the angular velocity to be zero, one may take more attention to the basin when the initial angular velocity is zero. For example, in this experiment, if the information on the basin is known as in Fig. 7h for $f = 1.15\,\mathrm{Hz}$, then we can surely get the anti-phase dynamics by pulling the swinging rod to a certain point of angle (less than $\pi/2$) and then releasing it from the stationary state. However,

the final state is hard to predict when the basins are riddled since tiny noise tends to change the fate of the final state (Aguirre and Sanjuan, 2002), for example, if we initially pull the rod to a position between $\theta = [\pi, 1.5\pi]$ for $f = 1.15$ Hz, the final state is possible in-phase or anti-phase in the experiment with small noise.

Owing to the interweave of basins of different states and inevitable systematic noise as well as experimental error, it is wise to calculate the basin stability based on the method presened by Menck *et al.* (2013). Applying it, we can calculate the basin stability for the anti-phase S_{BA} and in-phase pattern S_{BI} by estimating the volume of the basin in a relatively sensitive subset of the state volume $Q \in (\theta, \dot{\theta})$. Therefore, according to the basin stability for different parameters, the possibility of the system to reach the final state can be easily determined by the following forms

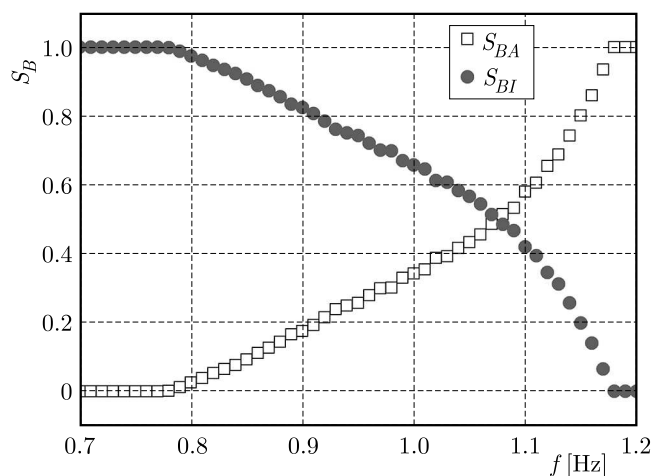$$S_{BA} = \frac{Vol(B_A \cap Q)}{Vol(Q)} \qquad S_{BI} = \frac{Vol(B_I \cap Q)}{Vol(Q)}$$

Fig. 8. Basin stability of the system

The basin stabilities of the two coexisting patterns of the system versus the driving frequency f are calculated with the subset volume $Q = 50000$ points for each $f \in [0.7, 1.2]$ Hz as shown in Fig. 8. When $f < 0.78$ Hz, all initial values will lead to an in-phase pattern. With an increment in the frequency f, the basin stability of the in-phase pattern continuously decreases till $f > 1.17$ Hz.

6. Conclusion

Experimental tests and nonlinear numerical analyses reveal a great deal of results that seem to be interesting from the research point of view. In this paper, a simple experimental device of a horizontally driven pendulum is set up to explore rich dynamics such as the bistability and bifurcation phenomenon in a specific range of the driving frequency. Two kinds of patterns, i.e. in--phase and anti-phase patterns coexisting with each other are observed. They have corresponding branches of amplitude-frequency characteristics. The riddled basins are observed, which makes it difficult to predict the final state in the experiment on a real system. The basin of stability is calculated and applied to predict the final states of the multi-stable system for different driving frequencies. When the driving frequency is low, the system has a unique in-phase oscillation state; the basin of stability of the in-phase state decreases with an increment in the driving frequency till the in-phase state disappears when the driving frequency is larger than a certain value.

Finally, we verified the experimental results by numerical simulation. Some suggestions were also brought out from theory, which facilitated in the experiment the controlling of the final state of the system and switching it between two kinds of oscillation states. Moreover, we hope that our study of the horizontally driven pendulum system can play a guiding role in thr control and synchronization problems of driven damping systems and coupled oscillatory systems in real life.

References

1. AGUIRRE J., SANJUAN M.A.F., 2002, Unpredictable behavior in the Duffing oscillator: Wada basins, *Physica D*, **171**, 1/2, 41-51

2. BAKER G.L., 1995, Control of the chaotic driven pendulum, *American Journal of Physics*, **63**, 9, 832-838

3. HENG H., MARTIENSSEN W., 1992, Analysing the chaotic motion of a driven pendulum, *Chaos, Solitons and Fractals*, **2**, 3, 323-334

4. LEVEN R.W., KOCH B.P., 1981, Chaotic behavior of paramentrically excited damped pendulum, *Physics Letters A*, **86**, 2, 71-74

5. MASOUD Z.N., NAYFEH A.H., MOOK D.T., 2004, Cargo pendulation reduction of ship-mounted cranes, *Nonlinear Dynamics*, **35**, 3, 299-311

6. MENCK P.J., HEITZIG J., MARWAN N., KURTHS J., 2013, How basin stability complements the linear-stability paradigm, *Nature Physics*, **9**, 2, 89-98

7. MOKHA A., CONSTANTINOU M.C., REINHORN A.M., ZAYAS V.A., 1991, Experimental study of friction-pendulum isolation systeme, *Journal of Ftructural Engineering*, **117**, 4, 1201-1217

8. NAKAMURA Y., SARUTA M., WADA A., TAKEUCHI T., HIKONE S., TAKAHASHI T., 2011, Development of the core-suspended isolation system, *Earthquake Engineering and Structural Dynamics*, **40**, 4, 429-447

9. SAUER I.M., FRANK J., BUCHERL E.S., 1999, Proposal of a new electromechanical total artificial heart: the TAH Serpentina, *Aritificial Organs*, **23**, 3, 290-291

10. SCHMITT J.M., BAYLY P.V., 1998, Bifurcations in the mean angle of a horizontally shaken pendulum: analysis and experiment, *Nonlinear Dynamics*, **15**, 1, 1-14

11. THAKUR R.B., ENGLISH L.Q., SIEVERS A.J., 2008, Driven intrinsic localized modes in a coupled pendulum array, *Journal of Physics D-Applied Physics*, **41**, 1, 015503

12. WU Y., SONG Z., LIU W., JIA J., XIAO J., 2014, Experimental and numerical study on the basin stability of the coupled metronomes, *European Physical Journal-Special Topics*, **223**, 4, 697-705

13. WU Y., WANG N.C., LI L.X., XIAO J., 2012, Anti-phase synchronization of two coupled mechanical metronomes, *Chaos*, **22**, 2, 5

14. WU Y., XIAO J.H., HU G., ZHAN M., 2012, Synchronizing large number of nonidentical oscillators with small coupling, *Europhysics Letters*, **97**, 4, 6

15. YAN X., TRISTRAM J.A., HARVINDER S.S., 2012, Instability dynamics of a horizontally shaken pendulum, *Australian and New Zealand Industrial and Applied Mathematics*, **53** (EMAC2011), C325-C339